An informational approach to the Network Disease Hypothesis in resting state fMRI

Jaime Gomez-Ramirez

Abstract Network theory approaches to brain connectivity in Resting-State fMRI have been mainly focused on the study of topological properties and network motifs that characterize the network structure. Small world architectures -highly clustered nodes connected thorough relatively short paths- have been identified in healthy and functional brain networks. It has been suggested that the disruption of normal brain function in diseases such as Schizophrenia and Alzheimer's disease, can be observed and measured in terms of variations in the network topology. For example, the reshaping of small-worldness into randomness in functional connectivity networks. However, a formal understanding of the interplay between brain disease and network connectivity is still missing. Here we combine network and information theory based approach to understand network robustness in Resting-State fMRI. We calculate the Kullback-Leibier distance between probability distribuions of the network before and after the deletion a node, and we compare this result with other studies on network vulnerability. A new theoretical framework for network robustness in Resting-State fMRI is provided.

Key words: brain function—bias — decision making — subjective value — utility function

1 Introduction

It has been suggested that fluctuations in the BOLD signal measured in humans in resting state, represent the neuronal activity baseline and shape spatially consistent patterns [37], [18]. These slow fluctuations in BOLD signal found in resting subjects, are highly coherent within either structural or functional networks in the

Universidad Politécnica de Madrid, Autonomous Systems Laboratory,
José Gutiérrez Abascal, 2 Madrid 28006, e-mail: jd.gomez@upm.es

human brain. Therefore, exploring these fluctuations could lead to a better understanding of the brain's intrinsic or spontaneous neural activity. Functional correlation based on the synchrony of low-frequency blood flow fluctuations in resting state, have been identified in the sensorimotor [25], visual [13], language [22], auditory [23], dorsal and ventral attention [16] and the frontoparietal control system [48]. The systematic study of those patterns using correlation analysis techniques has identified a number of resting state networks, which are functionally relevant networks found in subjects in the absence of either goal directed-task or external stimuli. The visual identification of the overall connectivity patters in resting state functional magnetic resonance imaging (RS-fMRI), has been assessed using either model-based and model-free approaches. In the former, statistical parametric maps of brain activation are built upon voxel-wise analysis location. This approach has been successful in the identification of motor networks, but it shows important limitations when the seed voxel cannot be easily identified. For example, in brain areas with unclear boundaries; i.e. cognitive networks involved for instance, in language or memory. Independent Component Analysis (ICA), on the other hand, is a model-free approach that allows separating resting fluctuations from other signal variations, resulting on a collection of spatial maps, one for each independent component, that represent functionally relevant networks in the brain. While ICA has the advantage over model-free methods that it is unbiased, (that is, it does not need to posit a specific temporal model of correlation between ROIs), the functional relevance of the different components is, however, computed relative to their resemblance to a number of networks based on criteria that are not easily formalized. More recently, researchers using graph-theory based methods have been able to not only visualize brain networks, but to quantify their topological properties. Large-scale anatomical connectivity analysis in the mammalian brain, shows that brain topology is neither random nor regular. Instead, it is organized in small world architectures [51], [44], characterized by high clustering and short path lengths. Small world networks are not solely structural, functional networks with a small world organization have been identified in the mammal brain [1]. In addition to this, disruptions in the small world organization can give clues about normal development and pathological conditions. For example, Supekar and colleagues [42] have shown that the deterioration of small world properties such as the lowering of the cluster coefficient, affect local network connectivity, which in turn may work as a network biomarker for Alzheimer's disease. Abnormalities in small-worldness may also have a significant positive correlation in, for example, schizophrenia [30] and epilepsy [29]. While network-based studies have been successful in delineating generic network properties, such as path length or clustering, additional work is needed in order to come to grips with the internal working of the systems underlying the network. Robustness in brain connectivity has been typically approached in terms of the impact that the complete disruption and/or removal of a network component has in the network topology [24]. However, by focusing on the topology of the network, factors that may play a key role in the network's vulnerability to failures can be neglected. For example, it has been suggested that patients with Alzheimer's disease show an increment in brain activity in certain areas relative to healthy subjects that compensates for the

disease related atrophy of other regions [39]. The network degeneration hypothesis, NDH for short, encompasses the idea that neuro degeneration can be studied as a network dysfunction process, in which changes in the network organization are informative about the progression of the disease [41], [35]. network-based approach to diagnosis of The network degeneration hypothesis -disease starts in small network assemblies, to progressively spread to connected areas of the initial locus- has been investigated in a number of brain pathologies including Alzheimer's disease [7], epilepsy [29], schizophrenia [30] and unipolar depression [31]. To our knowledge, the first attempt to systematically test the NDH is in [41], in which Seeley and colleagues use functional and structural network mapping approaches to characterize five distinct neurodegenerative syndromes.

In this paper we explore the network degeneration hypothesis using a methodology that combines graph and information theoretic tools. The Kullback-Leibler distance is here proposed as a measure of the network vulnerability relative to the suppression of certain nodes. It is shown that the nodes with higher Kullback-Leibler distance relative to the pre insult network represent critical elements to be targetted by the neural disease. This approach posits a new theoretical framework to investigate network robustness and how it is affected by internal perturbations such as aging and neurological disorders.

2 Materials and Methods

2.1 Subjects

Twenty-three healthy male volunteers (ages 21-32; mean 22.7) took part in the fMRI experiment. All subjects had normal or corrected-to-normal vision. The study was approved by the ethics committee of Okayama University, and written informed consent was obtained before the study.

2.2 Data acquisition

All subjects were imaged using a 1.5 T Philips scanner vision whole-body MRI system (Okayama University Hospital, Okayama, Japan), which was equipped with a head coil. Functional MR images were acquired during rest when subjects were instructed to keep their eyes closed and not to think of anything in particular. The imaging area consisted of 32 functional gradient-echo planar imaging (EPI) axial slices (voxel size=3x3x4 mm3, TR=3000 ms, TE=50 ms, FA=90^{o}, 64x64 matrix) that were used to obtain T2*-weighted fMRI images in the axial plane. We obtained 176 functional volumes and excluded the first 4 scans from analysis. Before the EPI scan, a T1-weighted 3D magnetization-prepared rapid acquisition gradient echo

(MP-RAGE) sequence was acquired (TR=2300 ms, TE=2.98 ms, TI=900 ms, voxel size=1x1x1 mm3).

2.3 Data preprocessing

Data were preprocessed using Statistical Parametric Mapping software SPM8 [] and REST v1.7 []. To correct for differences in slice acquisition time, all images were synchronized to the middle slice. Subsequently, images were spatially realigned to the first volume due to head motion. None of the subjects had head movements exceeding 2.5 mm on any axis or rotations greater than 2.5^{o}. After the correction, the imaging data were normalized to the Montreal Neurological Institute (MNI) EPI template supplied with SPM8 (resampled to 2x2x2 mm3 voxels) [**?**]. In order to avoid artificially introducing local spatial correlation, the normalized images were not smoothed [**?**]. Finally, the resulting data were temporally band-pass filtered (0.01-0.08 Hz) to reduce the effects of low-frequency drifts and high-frequency physiological noises [**?**].

2.4 Anatomical parcellation

Before whole brain parcellation, several sources of spurious variance including the estimated head motion parameters, the global brain signal and the average time series in the cerebrospinal fluid and white matter regions were removed from the data through linear regression [**?**]. Then, the fMRI data were parcellated into 90 regions using an automated anatomical labeling template [**?**]. For each subject, the mean time series of each region was obtained by simply averaging the time series of all voxels within that region.

2.5 Brain network construction

To measure the functional connectivity among regions, we calculated the Pearson correlation coefficients between any possible pair of regional time series, and then obtained a temporal correlation matrix (90x90) for each subject. We applied Fisher's r-to-z transformation to improve the normality of the correlation matrix. Then, two-tailed one-sample t-tests were performed for all the possible 4005 [i.e. (90x89)/2] pairwise correlations across subjects to examine whether each inter-regional correlation significantly differed from zero [**?**]. A Bonferroni-corrected significance level of P¡0.001 was further used to threshold the correlation matrix into an adjacency matrix whose element was 1 if there was significant correlation between the two brain regions and 0 otherwise. Finally, an undirected binary graph was acquired in

which nodes represent brain regions and edges represent links between regions. We then study the connectivity distribution of the resulting adjacency matrix. From our analysis we exclude the possibility that the connectivity distribution follows a power law . The log-log plot of the nodes connectivity cumulative probability distribution (Figure 1) is a nonoptimal fit with a straight line (solid line)). The next step is to study whether the connectivity network is scale free or a small world network. Note that in small world networks degree distributions other than power law are possible. For example, a power law can be cut-off by a Gaussian or exponential distribution, which apparently is the above scenario for the tail (Figure1). However, the figure 1 shows that only in the middle of the distribution we may have something similar to a power law. The extremes show an exponential or Gaussian kind of signature. The figure 2 depicts a good fit between with a normal distribution but only for connectity values between 5 to 15.

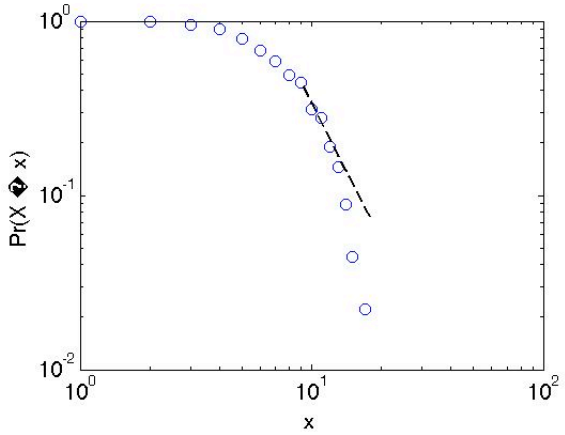

Fig. 1 Caption

In order to asses the network topology of the network depicted in Figure 3we need first to determine the randomized counterpart of the given network in order to relate the graph properties of the original network with those of the randomly built synthetic networks. Thus, the randomly built synthetic networks provide the null model that we need in order to identify whether the graph invariants in the real network are over represented or under represented in relation with the synthetic networks.

Here we explain how the generate a pool of randomly generated random network, then we compare the metric for the real network with this pool.

There are a number of different algorithms that may generate a pool of random network that maintain specific characteristics (graph invariants) that we wish the random network hold, such as connectivity degree, number of nodes, number of edges etc. First, we use the Renyi-Erdos model to provide a population of random

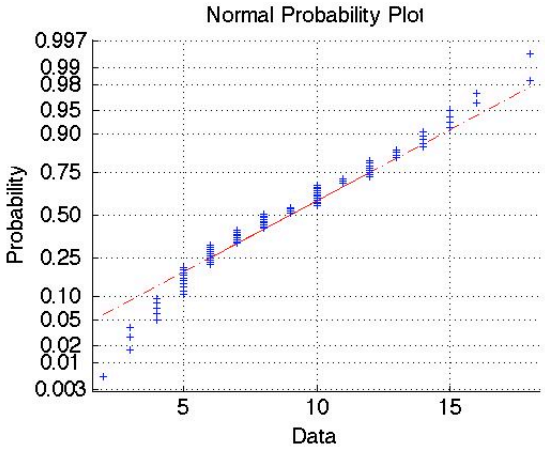

Fig. 2 Caption

networks with the same number of nodes and edges than the brain network (See Appendix for details). We obtain the global path length $\lambda = \frac{\lambda_{real}}{\lambda_{random}} = \frac{0.0881}{0.0993} = 0.8881$ and the local clustering coefficient is $\gamma = \frac{\gamma_{real}}{\gamma_{random}} = \frac{0.7790}{0.1005} = 7.7527$. Thus, $\sigma = \frac{\gamma}{\lambda} = 8.7299$, which indicates that the clustering tin the real network is much higher than in the counterpart random networks and the distance in the characteristic path length between the real and therandonly generated network is close to 1.

A different alternative to create random networks is using the Maslov's algorithm [34]. Here the degree of the nodes is preserved, that is, each node in the generated random network will have the same number of immediate neighbors. In the left side of Figure 4is shown the systematic deviations of the ratio $P(K0,K1)/P(K0,K1))$ from 1, and on the right side is depicted the statistical significance of the deviations. Both plots combined reveals regions on the plane were connections between brain regions are significantly enhanced or supressed compared to the null model. The red region in the left side plot indicates the tendency of poorly connected nodes to associate with other poorly connected nodes (less than four neighbors), blue regions in the upper left and lower right shows the reduced likelihood that highly connected nodes are directly linked with poorly connected nodes and viceversa. The Z scores plot on the right of Figure 4 is the normalized statistical significance of the deviations or $Z(K0,K1) = \frac{(P(K0,K1)-P(K0,K1)}{\sigma_r(K0,K1)}$, where $\sigma_r(K0,K1)$ is the the standard deviation of $P(K0,K1)$ in 100 realizations of a randomized network.

However, it might be emphasized that the empirical validation of the network degeneration hypothesis does not tell us much about the mechanisms that mediate in the alleged network connectivity sensitivity to neuropathological syndromes. A critical aspect is to understand network robustness, that is, functional network invariance under perturbation. In essence, robustness measures the capacity of the network to perform the same function before and after a perturbation. Perturbations

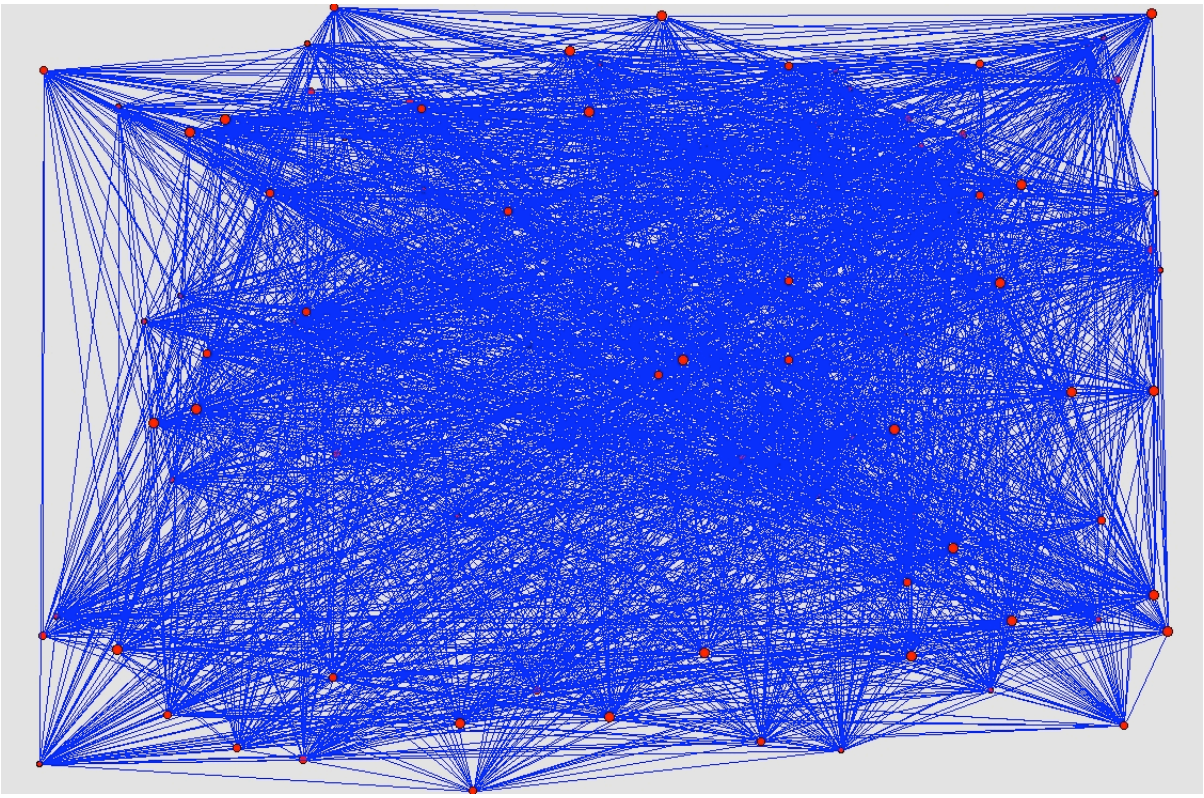

Fig. 3 Caption Pajek

are events, internal or external, that elicit a change in the network configuration, as for example in, to obliterate a node or a change in the connectivity between nodes. Thus, for a given network $G(V,E)$ with an adjacency matrix T, a perturbation d_A that transforms T into a new adjacency matrix T_A is given by the stochastic map $d_A : T \longrightarrow T_A$. Here, we assume that the perturbation d_A refers to the set of nodes that remained after having deleted the set of nodes $V - A$. Therefore, originally the network $G(V,E)$ is transformed into $G(A,E^A)$, where E^A are the remaining edge that results of eliminate the nodes $V - A$ from V. We want to measure the network vulnerability, to do so we calculate the geodesic path distance between any two nodes in the graph. The network efficiency is calculated using the Latora and Marchiori network efficiency measure [26]. The efficiency of the graph G, E(G) is :

$$E(G) = \frac{1}{n(n-1)\sum_{i \neq j \in G(N)} \frac{1}{d_{ij}}} \tag{1}$$

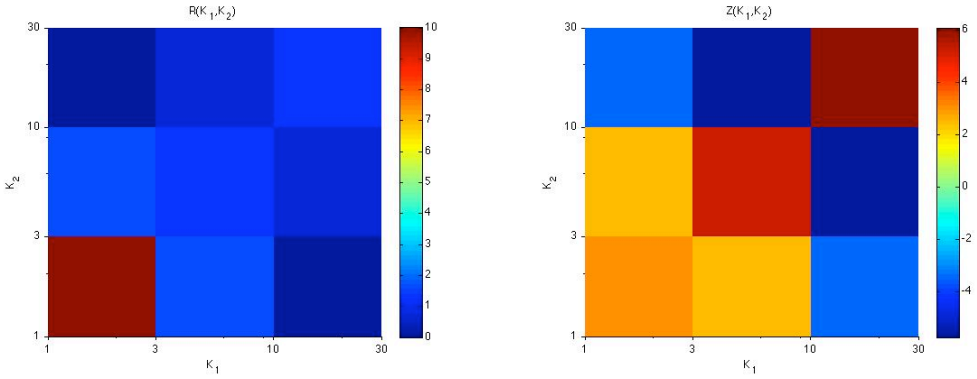

Fig. 4 Caption

where n is the number of nodes in $G(N)$ and dij is the shortest path length (the geodesic distance) between nodes i and j. The efficiency measure $E(G)$ is a network centrality measure that quantifies how the network efficiency if transmitting information deteriorates once a node is removed from the network. According to 1 a network is considered to be more efficient if the distances between pairs of nodes are smaller. Note that $0 \leq d_{ij} = d_{ji} \leq 1$. The global network efficiency is 0.3795 is a quite robust network , because young subjects? We can, furthermore, calculate the ranking of vulnerability of each node. The vunerability of node i, $vul(i)$ represents how the deletion of the node i affects the global efficiency of the resulting network and is given by the expression:

$$Vul(i) = \frac{E(G(N)) - E(G(N-i))}{E(G)} \tag{2}$$

In Table **??** is shown the vulnerability value for each of the AAL regions and their Broadmann area. Interestingly, there are some nodes that when removed, the

overall network vulnerability decreased -nodes 89 to 57 in the table. The deletion of node 89 results in an increase in the overall network efficiency of a 22.7% according to formula 2. The network vulnerability deteriorates for the the remaining 63 nodes. The worst performance occurred when nodes 60, 31, 50, 46, 73 and 30 are deleted in which case vulnerability of the ovrall resulting netwoirk is increased between 20% and 10%.

2.6 KL

Contrary to standard robustness studies reviewed in section **??** that measure the effect of network insults -typically node removal- in terms of macroscopic properties such as cost, efficiency or entropy, here we focus on the different adaptive processes that may follow the network disruption, and we are able to identify the strategies that promote function invariance. The Kullback-Leibler distance allows to answer the question of which of a set of approximating models is closest to the original model f. This is a classical problem of model selection in which the Kullback-Leibler distance allows elucidate which model in a set of candidate models, $g(x|\theta)$, is the closest to the true model $f(x)$. Accordingly, the best candidate is that with minimum distance. Thus, the minimum distance between f and g in the case of discrete distributions is given by:

$$KL(f,g) = \sum_{i=1}^{n} p_i \log(\frac{p_i}{q_i}) \tag{3}$$

where n is the number of possible outcomes of the underlying random variable, p_i is the probability distribution of the ith outcome and q_i is the approximating probability distribution. The KL distance is not a true metric since is not symmetric, as the distance is different from the distance. For a more in detailed description of KL, see [12]

It is important to note that KL cannot be computed unless we have a full knowledge of both the true model f and the parameters θ in g_θ. While this requirement is often unrealistic for observational studies, specially in biology, it holds in the present case [9]. The applicability of this approach relies upon the fact that "true model" f is given by the network adjacency matrix T prior to the insult d_A and the parameters θ in g_θ can be assigned to a vector $b_i = b_{i1}, \ldots, b_{i|A|}$ that assigns specific weights to each node in T_A, the resulting adjacency matrix of the perturbation d_A readjusted with a bias or strategy b_i, in which the passage through certain nodes are favored related to others. For example, a bias or adaptive strategy in which random walkers are more likely to visit nodes with highest betweenness centrality can be constructed straight forward by increasing the weight of the edges that lead to those nodes.

3 Results

4 Discussion

Traditionally, in task-related studies the resting state is assumed to be the baseline or control state with no functional significance. Recent advances in fMRI techniques have drastically challenged this view and have showed that "the baseline state of the brain is by no means an inactive state" (Damoiseaux, 2006). These slow fluctuations in BOLD signal found in resting subjects, are highly coherent within either structural or functional networks in the human brain. Therefore, exploring these fluctuations could lead to a better understanding of the brain's intrinsic or spontaneous neural activity. How these network properties are modified during normal development, aging or pathological conditions is still under debate. For example, it is unclear whether Alzheimer's disease affects local or global connectivity, or if connectivity is attenuated as in the Default Mode Network (DMN) (Greicius et al., 2004) or on the contrary, Alzheimer's disease may induce an increase in functional connectivity that compensates for the disease related atrophy of affected regions (Sanz-Arigita,2010).

RS- fMRI have been successfully used in classification of subjects with AD and MCI versus healthy controls. Connectivity changes in the default mode network can be used as markers of pathological conditions. For example, patients with tivity in the salience network. Alzheimer disease demonstrated decreased connectivity in the default mode network but increased connectivity in the salience network. Other studies rather than focusing on specific RSNs -default mode network- investigate altered connectivity patterns at a brain-wide level. The hypothesis that neurological disorders target large-scale functional and structural networks [41] rather than specific loci or sub-networks, calls for an integrative network-based approach.

Schizophrenia patients show a decreased functional connectivity during rest [28] suggesting a suboptimal information integration between regions of the brain network [36] AD patients show clustering coefficients significantly lower in patients compared with controls. There is a growing body of evidence that neurodegenerative disease targets specific large-scale brain networks, and clinical applications. Altered resting-state functional connectivity patterns have been shown in an impressive range of pathologies and conditions - Alzheimer's disease, schizophrenia, multiple sclerosis, Parkinson's disease, depression, autism, and even attention deficit/ hyperactivity disorder. See [27] for a review on clinical applications of rs-fMRI at the single subject level.

Despite the variability in the data acquisition protocols, statistical data analysis and gropus of subjects employed by different researchers, the litterature consistenly shows an overlap of functionally linked networks in the brain during resting state. The most commonly reported resting state networks are at least eight: the primary sensorimotor network, the primary visual and extra-striate visual network, bilateral temporal/insular and anterior cingulate cortex regions, left and right lateralized net-

works consisting of superior parietal and superior frontal regions, and the default mode network [46].

The method that study BOLD fluctuations that spontaneously emerge during awake rest is called resting state fMRI (R-fMRI), and the networks that are identified with such a methodology are resting state networks (RSNs). Resting state networks have been identified in a panoply of imaging techniques including fMRI [4], PET [38] (first identification of the Default Mode Network), near-infrared spectroscopy (NIRS) [40], EEG [33], [6] and fMRI combined with diffusion-based studies -diffusion tensor imaging (DTI) [47] and high angular resolution diffusion imaging (HARDI) [32]. Data analysis of resting state data falls into two gropus: seed-based and model-free methods. In the former, a functional connectivity map of regions of interest or seeds is obtained. The map represents the correlation between the resting-state time-series of the different seeds, which have been a priori selected [11], [17], [8], [5]. Model-free methods also provide a connectivity map across brain regions, but here the regions of interest are obtained through statistical analysis, rather than defined a priori as in the mode-based approach. A number of model-free computational tools exist to analyse resting-state time series, including independent component analysis [3] , [14], , clustering [43], [45] and machine learning techniques such as support vector machines [31], [52]. For a critique on the use of the "minimal assumption" adopted in model-free approaches such as ICA in neuroimage data analysis, see [19].

Seed-based methods are relatively straight forward to use and conteptually simple. A disadvantage is that the functional connectivity map here obtained is strictely dependent on the regions of interest previosly selected, overlooking the rest of brain areas and therefore falling to notice potentially relevant functional connection patterns. Model-free methods, on the other hand, explore functional connectivity at whole-brain scale. Independent component analysis allows direct comparison between subject groups [10], but presents the disadventage that it provides a number of different networks (components) whose biological relevance and consistency with previous findings need to be validated by other means. Note that model-based approaches avoid this dificulty by adopting the seeds or regions of interest a priori, either by selecting the relevant regions from a separate fMRI in a task experiment, or using a brain atlas in rest activity studies [49], [15].

Clustering and machine learning methods e.g., SVM, allow individual-based classification analysis. This is an important advantage to traditional group analyses of variance, and may bring important insights into disease onset prediction on individual subject basis [50]. Importantly, the above described approaches taken together show consistency in their results, that is, the functional maps tend to overlap across resting-state studies in the human brain [46].

It is important to realize that resting state networks are not the same as intrinsic connectivity networks (ICNs), which refer to network or components identified through multivariate decomposition statistical analysis e.g., independent component analysis (ICA), that show synchronous fluctuations during task performance. Therefore, RSNs are a sub class of ICNs which comprehend a set of large-scale func-

tionally connected brain networks not only in resting state but also in task-based neuroimaging data.

4.1 Graph Theory:a brain-scale approach

Until the recent advent of graph theoretic methods in RS-fMRI, the focus was put on the identification of anatomically separated regions that show a high level of functional correlation during rest. Grapth theory provides a theoretical framework to investigate the overall architecture of the brain. Thus, the emphasis has shifted from the identification of local subnetworks -default mode network, primary sensory motor network etc.- to the assesment of the topological and informational characteristics of a brain-scale complex network. The tools we use to model a system may also convey an ontological version of it, that is to say, the system under study is seen through the lens of a specific approach that necessarly shapes the observability domain. Thus, the identification of different subnetworks during rest can be seen as a by-product of the techniques used, for example identification component analysis (ICA) or clustering. On the other hand, the emphasis on the overall brain functional architecture might not suprised when using graph theoretic methods. Notable proponents of a modularist vision of brain connectivity to understand cognition -[21], [20]- have shifted toward a network-based approach- [2].

R-fMRI studies avoids the problem of task-evoked BOLD fluctuations and is easier to implement in subjects with their cognitive or motor capabilities reduced as in Alzheimer's or Parkinsons's disease.

References

1. D. S. Bassett and E. Bullmore. Small-world brain networks. *The Neuroscientist*, 12(6):512–523, Dec. 2006.
2. D. S. Bassett and M. S. Gazzaniga. Understanding complexity in the human brain. *Trends in cognitive sciences*, 15(5):200–209, May 2011. PMID: 21497128.
3. C. F. Beckmann, M. DeLuca, J. T. Devlin, and S. M. Smith. Investigations into resting-state connectivity using independent component analysis. *Philosophical transactions of the Royal Society of London. Series B, Biological sciences*, 360(1457):1001–1013, May 2005. PMID: 16087444.
4. B. Biswal, F. Z. Yetkin, V. M. Haughton, and J. S. Hyde. Functional connectivity in the motor cortex of resting human brain using echo-planar MRI. *Magnetic resonance in medicine: official journal of the Society of Magnetic Resonance in Medicine / Society of Magnetic Resonance in Medicine*, 34(4):537–541, Oct. 1995. PMID: 8524021.
5. R. Bluhm, P. Williamson, R. Lanius, J. Théberge, M. Densmore, R. Bartha, R. Neufeld, and E. Osuch. Resting state default-mode network connectivity in early depression using a seed region-of-interest analysis: Decreased connectivity with caudate nucleus. *Psychiatry and Clinical Neurosciences*, 63(6):754â761, 2009.
6. M. Boersma, D. J. A. Smit, H. M. A. de Bie, G. C. M. Van Baal, D. I. Boomsma, E. J. C. de Geus, H. A. Delemarre-van de Waal, and C. J. Stam. Network analysis of resting state

EEG in the developing young brain: structure comes with maturation. *Human brain mapping*, 32(3):413–425, Mar. 2011. PMID: 20589941.

7. R. L. Buckner, J. Sepulcre, T. Talukdar, F. M. Krienen, H. Liu, T. Hedden, J. R. Andrews-Hanna, R. A. Sperling, and K. A. Johnson. Cortical hubs revealed by intrinsic functional connectivity: mapping, assessment of stability, and relation to alzheimer's disease. *The Journal of neuroscience: the official journal of the Society for Neuroscience*, 29(6):1860–1873, Feb. 2009. PMID: 19211893.
8. R. L. Buckner and J. L. Vincent. Unrest at rest: default activity and spontaneous network correlations. *NeuroImage*, 37(4):1091–1096; discussion 1097–1099, Oct. 2007. PMID: 17368915.
9. K. P. Burnham and D. R. Anderson. *Model Selection and Multi-Model Inference: A Practical Information-Theoretic Approach*. Springer, Dec. 2010.
10. S. Chen, T. J. Ross, W. Zhan, C. S. Myers, K.-S. Chuang, S. J. Heishman, E. A. Stein, and Y. Yang. Group independent component analysis reveals consistent resting-state networks across multiple sessions. *Brain research*, 1239:141–151, Nov. 2008. PMID: 18789314 PMCID: PMC2784277.
11. D. Cordes, V. M. Haughton, K. Arfanakis, G. J. Wendt, P. A. Turski, C. H. Moritz, M. A. Quigley, and M. E. Meyerand. Mapping functionally related regions of brain with functional connectivity MR imaging. *AJNR. American journal of neuroradiology*, 21(9):1636–1644, Oct. 2000. PMID: 11039342.
12. T. M. Cover and J. A. Thomas. *Elements of Information Theory*. Wiley-Interscience, Aug. 1991.
13. J. S. Damoiseaux, S. A. R. B. Rombouts, F. Barkhof, P. Scheltens, C. J. Stam, S. M. Smith, and C. F. Beckmann. Consistent resting-state networks across healthy subjects. *Proceedings of the National Academy of Sciences of the United States of America*, 103(37):13848–13853, Sept. 2006. PMID: 16945915.
14. M. De Luca, C. F. Beckmann, N. De Stefano, P. M. Matthews, and S. M. Smith. fMRI resting state networks define distinct modes of long-distance interactions in the human brain. *NeuroImage*, 29(4):1359–1367, Feb. 2006. PMID: 16260155.
15. A. V. Faria, S. E. Joel, Y. Zhang, K. Oishi, P. C. M. van Zjil, M. I. Miller, J. J. Pekar, and S. Mori. Atlas-based analysis of resting-state functional connectivity: evaluation for reproducibility and multi-modal anatomy-function correlation studies. *NeuroImage*, 61(3):613–621, July 2012. PMID: 22498656.
16. M. D. Fox, M. Corbetta, A. Z. Snyder, J. L. Vincent, and M. E. Raichle. Spontaneous neuronal activity distinguishes human dorsal and ventral attention systems. *Proceedings of the National Academy of Sciences of the United States of America*, 103(26):10046–10051, June 2006. PMID: 16788060.
17. P. Fransson. Spontaneous low-frequency BOLD signal fluctuations: an fMRI investigation of the resting-state default mode of brain function hypothesis. *Human brain mapping*, 26(1):15–29, Sept. 2005. PMID: 15852468.
18. P. Fransson. How default is the default mode of brain function?: Further evidence from intrinsic BOLD signal fluctuations. *Neuropsychologia*, 44(14):2836–2845, 2006.
19. K. J. Friston. Modes or models: a critique on independent component analysis for fMRI. *Trends in Cognitive Sciences*, 2(10):373–375, Oct. 1998.
20. J. Fuster. The module: crisis of a paradigm book review, "the new cognitive neurosciences" 2nd edition, m.s. gazzaniga, editor-in-chief, mit press. *Neuron*, (26):51–53, 2000.
21. M. S. Gazzaniga, editor. *The New Cognitive Neurosciences: Second Edition*. The MIT Press, 2 edition, Nov. 1999.
22. M. Hampson, B. S. Peterson, P. Skudlarski, J. C. Gatenby, and J. C. Gore. Detection of functional connectivity using temporal correlations in MR images. *Human brain mapping*, 15(4):247–262, Apr. 2002. PMID: 11835612.
23. M. D. Hunter, S. B. Eickhoff, T. W. R. Miller, T. F. D. Farrow, I. D. Wilkinson, and P. W. R. Woodruff. Neural activity in speech-sensitive auditory cortex during silence. *Proceedings of the National Academy of Sciences of the United States of America*, 103(1):189–194, Jan. 2006. PMID: 16371474.

24. M. Kaiser, R. Martin, P. Andras, and M. P. Young. Simulation of robustness against lesions of cortical networks. *European Journal of Neuroscience*, 25(10):3185–3192, 2007.
25. S.-M. Kokkonen, J. Nikkinen, J. Remes, J. Kantola, T. Starck, M. Haapea, J. Tuominen, O. Tervonen, and V. Kiviniemi. Preoperative localization of the sensorimotor area using independent component analysis of resting-state fMRI. *Magnetic resonance imaging*, 27(6):733–740, July 2009. PMID: 19110394.
26. V. Latora and M. Marchiori. Efficient behavior of small-world networks. *Physical Review Letters*, 87(19):198701, Oct. 2001.
27. M. H. Lee, C. D. Smyser, and J. S. Shimony. Resting-state fMRI: a review of methods and clinical applications. *AJNR. American journal of neuroradiology*, Aug. 2012. PMID: 22936095.
28. M. Liang, Y. Zhou, T. Jiang, Z. Liu, L. Tian, H. Liu, and Y. Hao. Widespread functional disconnectivity in schizophrenia with resting-state functional magnetic resonance imaging. *Neuroreport*, 17(2):209–213, Feb. 2006. PMID: 16407773.
29. W. Liao, Z. Zhang, Z. Pan, D. Mantini, J. Ding, X. Duan, C. Luo, G. Lu, and H. Chen. Altered functional connectivity and small-world in mesial temporal lobe epilepsy. *PLoS ONE*, 5(1):e8525, Jan. 2010.
30. Y. Liu, M. Liang, Y. Zhou, Y. He, Y. Hao, M. Song, C. Yu, H. Liu, Z. Liu, and T. Jiang. Disrupted small-world networks in schizophrenia. *Brain: a journal of neurology*, 131(Pt 4):945–961, Apr. 2008. PMID: 18299296.
31. A. Lord, D. Horn, M. Breakspear, and M. Walter. Changes in community structure of resting state functional connectivity in unipolar depression. *PLoS ONE*, 7(8):e41282, Aug. 2012.
32. M. J. Lowe, E. B. Beall, K. E. Sakaie, K. A. Koenig, L. Stone, R. A. Marrie, and M. D. Phillips. Resting state sensorimotor functional connectivity in multiple sclerosis inversely correlates with transcallosal motor pathway transverse diffusivity. *Human brain mapping*, 29(7):818–827, July 2008. PMID: 18438889.
33. D. Mantini, M. G. Perrucci, C. D. Gratta, G. L. Romani, and M. Corbetta. Electrophysiological signatures of resting state networks in the human brain. *Proceedings of the National Academy of Sciences*, 104(32):13170–13175, Aug. 2007.
34. S. Maslov and K. Sneppen. Specificity and stability in topology of protein networks. *arXiv:cond-mat/0205380*, May 2002. Science, 296, 910-913 (2002).
35. M. Mesulam. Defining neurocognitive networks in the BOLD new world of computed connectivity. *Neuron*, 62(1):1–3, Apr. 2009. PMID: 19376059.
36. S. Micheloyannis, E. Pachou, C. J. Stam, M. Breakspear, P. Bitsios, M. Vourkas, S. Erimaki, and M. Zervakis. Small-world networks and disturbed functional connectivity in schizophrenia. *Schizophrenia research*, 87(1-3):60–66, Oct. 2006. PMID: 16875801.
37. M. E. Raichle and D. A. Gusnard. Intrinsic brain activity sets the stage for expression of motivated behavior. *The Journal of Comparative Neurology*, 493(1):167–176, 2005.
38. M. E. Raichle, A. M. MacLeod, A. Z. Snyder, W. J. Powers, D. A. Gusnard, and G. L. Shulman. A default mode of brain function. *Proceedings of the National Academy of Sciences of the United States of America*, 98(2):676–682, Jan. 2001. PMID: 11209064.
39. E. J. Sanz-Arigita, M. M. Schoonheim, J. S. Damoiseaux, S. A. R. B. Rombouts, E. Maris, F. Barkhof, P. Scheltens, and C. J. Stam. Loss of 'small-world' networks in alzheimer's disease: graph analysis of FMRI resting-state functional connectivity. *PloS One*, 5(11):e13788, 2010. PMID: 21072180.
40. S. Sasai, F. Homae, H. Watanabe, A. T. Sasaki, H. C. Tanabe, N. Sadato, and G. Taga. A NIRS-fMRI study of resting state network. *NeuroImage*, 63(1):179–193, Oct. 2012. PMID: 22713670.
41. W. W. Seeley, R. K. Crawford, J. Zhou, B. L. Miller, and M. D. Greicius. Neurodegenerative diseases target large-scale human brain networks. *Neuron*, 62(1):42–52, Apr. 2009. PMID: 19376066.
42. K. Supekar, V. Menon, D. Rubin, M. Musen, and M. D. Greicius. Network analysis of intrinsic functional brain connectivity in alzheimer's disease. *PLoS Computational Biology*, 4(6), June 2008. PMID: 18584043 PMCID: PMC2435273.
43. B. Thirion, S. Dodel, and J.-B. Poline. Detection of signal synchronizations in resting-state fMRI datasets. *NeuroImage*, 29(1):321–327, Jan. 2006. PMID: 16129624.

44. M. J. Vaessen, P. A. M. Hofman, H. N. Tijssen, A. P. Aldenkamp, J. F. A. Jansen, and W. H. Backes. The effect and reproducibility of different clinical DTI gradient sets on small world brain connectivity measures. *NeuroImage*, 51(3):1106–1116, July 2010. PMID: 20226864.
45. M. van den Heuvel, R. Mandl, and H. Hulshoff Pol. Normalized cut group clustering of resting-state fMRI data. *PLoS ONE*, 3(4):e2001, Apr. 2008.
46. M. P. van den Heuvel and H. E. Hulshoff Pol. Exploring the brain network: a review on resting-state fMRI functional connectivity. *European neuropsychopharmacology: the journal of the European College of Neuropsychopharmacology*, 20(8):519–534, Aug. 2010. PMID: 20471808.
47. M. P. van den Heuvel, R. C. W. Mandl, R. S. Kahn, and H. E. Hulshoff Pol. Functionally linked resting-state networks reflect the underlying structural connectivity architecture of the human brain. *Human brain mapping*, 30(10):3127–3141, Oct. 2009. PMID: 19235882.
48. J. L. Vincent, I. Kahn, A. Z. Snyder, M. E. Raichle, and R. L. Buckner. Evidence for a frontoparietal control system revealed by intrinsic functional connectivity. *Journal of neurophysiology*, 100(6):3328–3342, Dec. 2008. PMID: 18799601.
49. J. Wang, L. Wang, Y. Zang, H. Yang, H. Tang, Q. Gong, Z. Chen, C. Zhu, and Y. He. Parcellation-dependent small-world brain functional networks: a resting-state fMRI study. *Human brain mapping*, 30(5):1511–1523, May 2009. PMID: 18649353.
50. Y. Wang, Y. Fan, P. Bhatt, and C. Davatzikos. High-dimensional pattern regression using machine learning: from medical images to continuous clinical variables. *NeuroImage*, 50(4):1519–1535, May 2010. PMID: 20056158.
51. S. S. Watts D.J. Collective dynamics of 'small-world' networks. *Nature*, 393:2440442, 1998.
52. L.-L. Zeng, H. Shen, L. Liu, L. Wang, B. Li, P. Fang, Z. Zhou, Y. Li, and D. Hu. Identifying major depression using whole-brain functional connectivity: a multivariate pattern analysis. *Brain*, Mar. 2012.